Asymmetry-induced electric current rectification in permselective systems

Yoav Green,[*] Yaron Edri,[*] and Gilad Yossifon[†]
Faculty of Mechanical Engineering, Micro- and Nanofluidics Laboratory, Technion - Israel Institute of Technology, Technion City 32000, Israel
(Received 7 July 2015; published 30 September 2015)

For a symmetric ion permselective system, in terms of geometry and bulk concentrations, the system response is also symmetric under opposite electric field polarity. In this work we derive an analytical solution for the concentration distribution, electric potential, and current-voltage response for a four-layered system comprised of two microchambers connected by two permselective regions of varying properties. It is shown that any additional asymmetry in the system, in terms of the geometry, bulk concentration, or surface charge property of the permselective regions, results in current rectification. Our work is divided into two parts: when both permselective regions have the same surface charge sign and the case of opposite signs. For the same sign case we are able to show that the system behaves as a dialytic battery while accounting for field-focusing effects. For the case of opposite signs (i.e., bipolar membrane), our system exhibits the behavior of a bipolar diode where the magnitude of the rectification can be of order 10^2-10^3.

DOI: 10.1103/PhysRevE.92.033018 PACS number(s): 47.65.−d, 47.57.jd, 66.10.Ed, 82.39.Wj

I. INTRODUCTION

Permselective media such as nanoporous membranes or nanochannels possess a symmetry-breaking property—permselectivity—that allows preferential passage of charge carriers of one sign over the charge carrier of the opposite sign. Thus, under the application of an external electric potential or electrical current, the transport of ions through such media exhibit a preferred direction in forming concentration gradients within the system. On one end of the system a region depleted of ions is formed while at the other end an enriched region is formed. The formation of these concentrations gradients is determined by a steady-state current-voltage ($I-V$) response, which accounts for the numerous properties of the system including the geometry, the bulk concentration, and the surface charge properties of the permselective media [1,2]. The formation of these concentration gradients and the resultant $I-V$ relation are collectively termed concentration polarization (CP). The steady-state response of the system is of much importance and is used to characterize the systems, such as the conductance in the Ohmic region [3–5] or the diffusion-limited current of the system [6,7].

Understanding CP is of much importance as it is the governing physical mechanism in electrodialysis (ED) desalination systems ([8,9] and references therein) where under the application of an external electric field salts are removed from one desalted stream into another brine stream. In this context, desalination systems have received a lot of attention where much of the emphasis was on the nonlinear response due to the formation of an extended space-charge layer (SCL) [10], surface conduction [11,12], and numerous electroconvective mechanisms [13–18]. The analysis in these works analyzed the effects in single microchamber, which was usually one dimensional (1D) thus making the system homogenous. Recently, the linear [5,19,20] and nonlinear [21] effects were extended to the more realistic three-layered heterogeneous geometry encountered in numerous experiments [3,4,22–25], and simulation [25–27].

In contrast to an ED system, which operates under an applied electric current, a reverse-electrodialysis (RED) system works in the reverse *modus operandi*, an electric current is harvested due to asymmetric concentrations at the end of the system [28–30]. Such systems have also been termed dialytic batteries [29]. Numerous works, using varying and substantially different experimental setups [31–35], as well as numerical investigation [36,37], have shown that energy could be harvested through fresh water and seawater mixing. The key point to realize is the inherent potential to harvest energy at any location at which fresh water rivers pour into the oceans (approximately 2.2 kJ per liter of fresh water [28,29]). Regardless of mankind, physics dictates that the fresh water is going to flow into the ocean, the energy that is harvested is 100% green energy [38]. It has been estimated that amount of energy that can be harvested amounts to 2 TW, which is approximately 13% of the world's energy consumption [39]. Surprisingly, excluding the pioneering work of Weinstein and Leitz [29] (which treated membrane systems), little theoretical work has been conducted in this field. In nanochannel systems only initial experimental work has been conducted [40–42] but even in this aspect the full potential of these systems has not been fully realized. It may not be too surprising that such asymmetric systems have not received theoretical attention as up until recently most works focused on the one-layered systems and as such could not consider bulk concentration asymmetries specifically or any asymmetries in general. With the emergence of three-layered models [5,19,20], the need to address matters of asymmetries has become more pressing.

In this work we shall show that any asymmetries within a permselective system will cause current rectification. In their seminal work of Weinstein and Leitz [29] considered only a 1D system, where based on heuristic principles they derived a very clever and simple model for the resultant potential of a dialytic battery under a zero applied electric current without the effects of CP and with a number of fitting parameters. In this work we shall methodologically derive a complete solution, which not only includes the final $I-V$

[*]These authors contributed equally to this work.
[†]Corresponding author: yossifon@tx.technion.ac.il

relation but will also include the concentration and electric potential distributions. No fitting parameters are required in our model. Although the approach taken by us is not limited to the number of layers, for illustration purposes we have focused on a four-layered 2D system comprised of two microchannels connected by two permselective regions (where the geometry in each region can be different, Fig. 1) under the forcing of an external applied potential as well as asymmetric bulk concentrations. Understanding the effects of two dimensions (or three dimensions) is of much importance in permselective systems, which are inherently not 1D. The four-layer layout of such a system will allow us also to consider two additional asymmetries that have thus far received only initial consideration: (i) asymmetric permselective geometries [43,44] and (ii) asymmetric permselective charge properties. In an attempt to keep the introduction structured, we have thus far only provided a review of the first case. For the second case we will provide the introduction at the beginning of Sec. IV, which deals with the case of asymmetric permselective charge properties.

This work is divided in the following manner. In Sec. II we shall introduce the governing equations and describe the geometry. Section III focuses on a more standard four-layered system where both permselective regions are assumed to be ideally permselective and both regions are either cation or anion permselective. We derive a general solution and discuss the numerous consequences, which include rectification and energy harvesting. In Sec. IV. we focus on a four-layered system where each permselective region's surface charge is of different sign. Once more, we outline the model and its principle assumptions, derive the solution, and discuss the outcomes. We note that in Sec. IV the assumption of ideal permselection is lifted but another assumption is required for an analytical solution. Finally, concluding remarks are given in Sec. V.

II. GOVERNING EQUATIONS AND GEOMETRY

The nondimensional equations governing steady-state convectionless ion transport through a permselective medium for a symmetric and binary ($z_+ = -z_- = 1,\ \tilde{D}_+ = \tilde{D}_- = \tilde{D}$) electrolyte are the Poisson-Nernst-Planck (PNP) equations

$$\nabla \cdot (\nabla c_+ + c_+ \nabla \phi) = -\nabla \cdot \boldsymbol{j}_+ = 0, \tag{1}$$

$$\nabla \cdot (\nabla c_- - c_- \nabla \phi) = -\nabla \cdot \boldsymbol{j}_- = 0, \tag{2}$$

$$2\varepsilon^2 \nabla^2 \phi = -\rho_e, \tag{3}$$

wherein Eqs. (1) and (2) are the Nernst-Planck equations satisfying the continuity of ionic fluxes conditions. The decoupling of the electrodiffusive problem from the electroconvective problem in the underlimiting regime is based on the smallness of the Peclet number for inhomogeneous media [6,7]. The cationic and anionic concentrations, $\tilde{c}_+$ and $\tilde{c}_-$, respectively, have been normalized by one of the bulk concentrations, i.e., $\tilde{c}_0$ taken as either $\hat{c}_1$ or $\hat{c}_4$, where the tilde stands for the parameter in its dimensional form. The spatial coordinates have been normalized by the diffusion length (DL) $\tilde{L}$, the ionic fluxes have been normalized by $\tilde{D}\tilde{c}_0/\tilde{L}$. Equation (3) is the Poisson equation for the electric potential $\tilde{\phi}$, which has been normalized by the thermal potential $\Re T/F$, where $\Re$ is the universal gas constant, T is the absolute temperature, and F is the Faraday constant. The nondimensional charge density ρ_e, appearing in Eq. (3) is normalized by $zF\tilde{c}_0$. The normalized Debye layer is $\varepsilon = \tilde{\lambda}_D/\tilde{L}$, with

$$\tilde{\lambda}_D = \sqrt{\frac{\varepsilon_0 \varepsilon_r \Re T}{2F^2 \tilde{c}_0}}, \tag{4}$$

where ε_0 and ε_r are the permittivity of vacuum and the relative permittivity of the electrolyte, respectively. The space-charge density is given by the relation

$$\rho_e = c_+ - c_- - N_2\delta_{2,k} - N_3\delta_{3,k}, \tag{5}$$

where k represents the regions ($k = 1,2,3,4$, and see Fig. 1) and $\delta_{l,k}$ is Kronecker's δ ($l = 2,3$ will be used throughout this paper to denote the permselective regions). The properties for N_2 and N_3, which are the excess counterion concentrations in regions 2 and 3, will be defined differently as needed in Secs. III and IV.

Our model consists of a four-layered system in which two microchambers are connected by permselective mediums, wherein all four domains are of rectangular shape, as shown in Fig. 1. The left microchamber, termed "region 1", is defined in the domain $x \in [0,L_1], y \in [0,H_1]$. The permselective mediums, termed "region 2" and "region 3", are defined by the domains $x \in [L_1, L_1 + d_2], y \in [0,h_2]$ and $x \in [L_1 + d_2, L_1 + d_2 + d_3], y \in [0,h_3]$, respectively. The right microchamber, termed "region 4", is defined in the domain $x \in [L_1 + d_2 + d_3, L_1 + d_2 + d_3 + L_4], y \in [0,H_4]$. Such a geometry realistically describes systems that have been the subject of numerous recent experiments [41,43,44]. The spatial coordinates have been normalized by the DL length, $\tilde{L}$ ($\tilde{L}$ can be chosen arbitrarily as either $\tilde{L}_1$ or $\tilde{L}_4$ [5]). Without loss of generality, we shall formulate the solution for general values of the dimensionless L_1 and L_4 while we shall remember that at least one of these values when normalized is unity.

Under the local electroneutrality (LEN) approximation [1,2,10,14], one takes $\varepsilon = 0$, as a result of Eq. (3) $\rho_e = 0$. The implication will be discussed in each of the following sections separately.

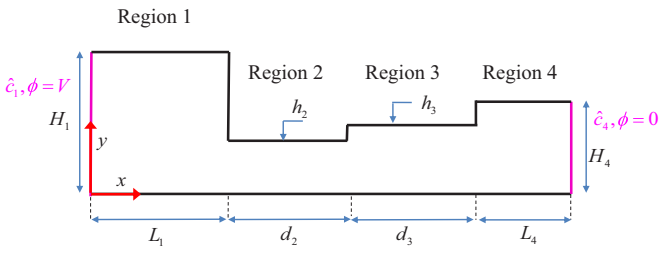

FIG. 1. (Color online) Schematic describing a two-dimensional four-layered system comprised of two microchambers (regions 1 and 4) connected by two permselective mediums (regions 2 and 3). The geometry of each region is described in the schematic while the surface charge properties (or the counterion concentrations) of the permselective regions are defined in Secs. III A and IV A. Black lines prescribe zero flux BC ($\boldsymbol{j}_\pm \cdot \boldsymbol{n} = 0, \partial\phi/\partial n = 0$) while the magenta lines at the two opposite ends $x = 0,\ \Delta_4$ prescribe Dirichlet BCs and are given in the schematic.

III. SYMMETRIC IDEAL PERMSELECTIVE REGIONS

In this section we will discuss the case where N_2 and N_3 are of the same sign. We will arbitrarily assume, without loss of generality, that they are positive. We assume that the media are ideally permselective, hence the transport of negatively charged ions through the interfaces is zero ($\boldsymbol{j}_- = 0$).

A. Assumptions

Under the LEN approximation, $\rho_e = 0$, within the microchambers (regions 1 and 4) the positive and negatively charged ion concentrations are equal ($c_+ = c_- = c$). Upon substitution of this into Eqs. (1) and (2), and taking its sum leads to

$$\nabla^2 c = 0. \tag{6}$$

From the careful inspection of the boundary conditions (BCs) in an ideal permselective system under steady-state conditions, the coion flux is zero everywhere ($\boldsymbol{j}_- \cdot \boldsymbol{n} = \boldsymbol{0}$) leading to [from Eq. (2)] [5–7]

$$\phi = \ln c + \bar{\phi}, \tag{7}$$

where $\bar{\phi}$ is an integration constant. The assumption of an ideal permselective medium usually corresponds to the case where $N_{2,3} \gg 1$ and the coion approximation is of order $\sim 1/N$. For ideal permselectivity, careful inspection of the BCs and the remaining assumptions leads to the approximation $c_{2,3+} \approx N_{2,3}, c_{2,3-} \approx 0$.

B. Boundary conditions

In this part we shall provide the appropriate BCs required for the solution of Eqs. (6)–(7) for this section. At the opposite ends of the system we require the concentrations to have a bulk value, which are not necessarily equal, and the potential drop over the entire system is V

$$c(x = 0) = \hat{c}_1, \quad c(x = \Delta_4) = \hat{c}_4, \tag{8}$$

$$\phi(x = 0) = V, \quad \phi(x = \Delta_4) = 0, \tag{9}$$

where $\Delta_4 = L_1 + d_2 + d_3 + L_4$ is the length of the entire system. It should be pointed out that the ideal permselective assumption requires that $\max(\hat{c}_1, \hat{c}_4) \ll \min(N_2, N_3)$. Requiring no penetration of ions ($\boldsymbol{j}_\pm \cdot \boldsymbol{n} = \boldsymbol{0}$, where n is the coordinate normal to the surface or symmetry plane) along with electrical insulation $\partial\phi/\partial n$ at the microchamber walls (or at the symmetry planes), translates into

$$\frac{\partial c}{\partial n} = 0. \tag{10}$$

This can be written explicitly as

$$c_y(x, H_k) = c_y(x, 0) = 0, \quad k = 1,4. \tag{11}$$

At the permselective medium surfaces located at $x = \Delta_1 = L_1, x = \Delta_2 = L_1 + d_2$, and $x = \Delta_3 = L_1 + d_2 + d_3$ we make a simplifying assumption of uniform current density along the permselective interface. We shall also require the continuity of the total electric current per unit width (in the z-coordinate direction), I (normalized by $F\tilde{D}\tilde{c}_0$), such that

$$c_x(x = \Delta_1, y) = \begin{cases} -I/(2h_2) & 0 \leqslant y \leqslant h_2, \\ 0 & \text{otherwise}, \end{cases} \tag{12}$$

$$c_x(x = \Delta_3, y) = \begin{cases} -I/(2h_3) & 0 \leqslant y \leqslant h_3, \\ 0 & \text{otherwise}, \end{cases} \tag{13}$$

$$@x = \Delta_2, \quad I = i_2 h_2 = i_3 h_3. \tag{14}$$

Equation (14) represents the requirement that the total electric current is conserved at the interface $x = \Delta_2$ where a discontinuity exists in the geometries thus leading to different electric current densities i_2, i_3 (normalized by $F\tilde{D}\tilde{c}_0/\tilde{L}$). To avoid ambiguity, we shall discuss the solutions only in terms of the current I itself. In the above equations we have used the simplifying assumption of uniform ionic current density along the interface between the permselective medium and the microchannels. The above-mentioned equations are satisfactory for the solution of the concentration distributions in each of the regions, which will be solved shortly.

We now provide the BCs required for the solution of the electric potential. At the interface between the regions, we require the continuity of the electrochemical potential

$$\mu_\pm(x, y) = \ln[c_\pm(x, y)] \pm \phi(x, y). \tag{15}$$

Within an ideal permselective medium, $c_- = 0$, leading to an infinite μ_-, thus we apply this condition only for μ_+. We require the continuity at three points along the centerline at the interfaces

$$\mu_{+,k}(x = \Delta_k, y = 0) = \mu_{+,k+1}(x = \Delta_k, y = 0), \quad k = 1,2,3. \tag{16}$$

C. Concentration solution

From Eqs. (6), (8), and (11)– (13), using the separations of variable technique, under the assumption of ideal permselectivity, one gets the two-dimensional concentration distribution

$$c_1(x, y) = \hat{c}_1 - \frac{I}{2H_1}x - \frac{I}{h_2 H_1}\sum_{n=1}^{\infty} \frac{\sin(\lambda_n h_2)}{\lambda_n^2 \cosh(\lambda_n L_1)} \sinh(\lambda_n x)\cos(\lambda_n y), \tag{17}$$

$$c_{+,2}(x, y) = N_2, \quad c_{-,2}(x, y) = 0, \tag{18}$$

$$c_{+,3}(x, y) = N_3, \quad c_{-,3}(x, y) = 0, \tag{19}$$

$$c_4(x, y) = \hat{c}_4 + \frac{I}{2H_4}(\Delta_4 - x) + \frac{I}{h_3 H_4}\sum_{n=1}^{\infty} \frac{\sin(\kappa_n h_3)}{\kappa_n^2 \cosh(\kappa_n L_4)} \sinh[\kappa_n(\Delta_4 - x)]\cos(\kappa_n y), \tag{20}$$

with

$$\lambda_n = \frac{\pi n}{H_1}, \quad \kappa_n = \frac{\pi n}{H_4}. \tag{21}$$

The first two terms in Eqs. (17) and (20) are the one-dimensional concentration distributions, which have been modified to have general bulk values. The third term accounts for the 2D distribution. For a complete discussion on the effects of the third term in Eqs. (17) and (20) see Refs. [5–7,19,20,45]. Of these works, only Refs. [5,19,20] focused on three-layered systems whereas here we provide a solution for a four-layered system, where the additional term appears rather trivial. The added bonus is that we account for asymmetric bulk concentrations as well as asymmetric permselective geometries (that is not possible in a three-layered system). All these asymmetries will lead to rectifications as we shall discuss shortly.

D. Electric potential solution

Using Eqs. (7) and (9) leads to the following electric potential distributions within the microchambers

$$\begin{aligned} \phi_1(x,y) &= \ln\left[\frac{c_1(x,y)}{\hat{c}_1}\right] + V, \\ \phi_4(x,y) &= \ln\left[\frac{c_4(x,y)}{\hat{c}_4}\right]. \end{aligned} \tag{22}$$

In contrast, in the ideal permselective regions 2 and 3, using Eq. (1) under the assumption of ideal permselectivity ($j_- = 0, j_+ = I/h$), yields the solution for the electric potential

$$\phi_2(x,y) = -\frac{I}{h_2 N_2}x + \bar{\phi}_2, \quad \phi_3 = -\frac{I}{h_3 N_3}x + \bar{\phi}_3. \tag{23}$$

Requiring continuity of the electrochemical potentials at the three interfaces [Eq. (16)] we find the two unknowns $\bar{\phi}_2$, $\bar{\phi}_3$ and a $I-V$ relation

$$\bar{\phi}_3 = \frac{I\Delta_3}{h_3 N_3} + 2\ln[c_4(x=\Delta_3, y=0)] - \ln(N_3\hat{c}_4), \tag{24}$$

$$\bar{\phi}_2 = \bar{\phi}_3 + \ln\left(\frac{N_3}{N_2}\right) + \frac{I\Delta_2}{h_2 N_2} - \frac{I\Delta_2}{h_3 N_3}, \tag{25}$$

$$\begin{aligned} V = {} & I\left(\frac{d_2}{h_2 N_2} + \frac{d_3}{h_3 N_3}\right) \\ & + 2\ln\left(\frac{\hat{c}_4 + \frac{I}{2H_4}L_4 + I\bar{f}_4}{\hat{c}_1 - \frac{I}{2H_1}L_1 - I\bar{f}_1}\right) - \ln\left(\frac{\hat{c}_4}{\hat{c}_1}\right), \end{aligned} \tag{26}$$

with

$$\bar{f}_1 = \frac{1}{h_2 H_1}\sum_{n=1}^{\infty}\frac{\sin(\lambda_n h_2)}{\lambda_n^2}\tanh(\lambda_n L_1), \tag{27}$$

$$\bar{f}_4 = \frac{1}{h_3 H_4}\sum_{n=1}^{\infty}\frac{\sin(\kappa_n h_3)}{\kappa_n^2}\tanh(\kappa_n L_4). \tag{28}$$

The $I-V$ relation given by Eq. (26) is comprised of three different terms. The first term represents the Ohmic resistance of the nanochannels. The second term is a nonlinear resistor that accounts for depletion and enrichment within the microchambers. The resistor also accounts for the field-focusing effects at the interfaces through the $\bar{f}_k$ functions. The behavior of the $\bar{f}_k$ functions in the varying limits of heterogeneity, i.e., large and small h/H, has been recently investigated [7]. In addition, the asymmetric bulk concentrations contribute in the following manner: (i) introduction of the third term in Eq. (26); (ii) playing an important role in the microchamber nonlinear resistance in the second term. In a system with symmetric bulk concentrations the depleted (enriched) region has a concentration that is lower (higher) than the bulk concentration. In principal, depending on the bulk values, geometry, and current bias, one can have that the enriched region will indeed have an interfacial concentration higher than the connecting reservoir's bulk value but it will still be lower than the depleted concentration at the opposite microchamber. A key point to realize from Eq. (26) is that any asymmetry (bulk concentration, geometric, or both) in the system will result in current rectification.

E. Analysis

We shall now elaborate on a number of these outcomes from an intuitive standpoint, after which we shall demonstrate the addressed points.

Energy harvesting. The final term in Eq. (26) results in the ability to harvest an electric current I_0 from the system without applying an external potential drop $V = 0$. If $\hat{c}_1 = \hat{c}_4 = 1$, then for reasons of symmetry, when the system is not forced, it is in equilibrium and thus the current is zero. In contrast, when $\hat{c}_1 \neq \hat{c}_4$, an inherent concentration gradient exists—due to a gradient in the electrochemical potential and the symmetry-breaking property of ion permselectivity. The existence of a concentration gradient requires that the current is nonzero. The exact value of I_0 needs to be solved by the transcendental equation of $V = 0$. It is clear that as the asymmetry $\hat{c}_1/\hat{c}_4$ is increased so will the harvested electrical current.

Limiting current. The limiting current, defined when the concentration within the microchannel interfacing the permselective medium is zero [Eqs. (17) or (20)], depends not only on the geometry but also on the on the bulk concentrations

$$I_{\mathrm{lim},1} = \hat{c}_1 \Big/ \left(\frac{L_1}{2H_1} + \bar{f}_1\right), \tag{29}$$

$$I_{\mathrm{lim},4} = -\hat{c}_4 \Big/ \left(\frac{L_4}{2H_4} + \bar{f}_4\right). \tag{30}$$

It is observed that even for a symmetric geometry about $x = \Delta_2$ ($h_2 = h_3$, $d_2 = d_3$, $H_1 = H_4$, $L_1 = L_4$), the asymmetric bulk concentrations would lead to asymmetric limiting currents.

Conductance. We can look at the current response for small currents $I \ll 1$,

$$\begin{aligned} V = {} & I\left(\frac{d_2}{h_2 N_2} + \frac{d_3}{h_3 N_3} + \frac{L_1}{\hat{c}_1 H_1} + 2\frac{\bar{f}_1}{\hat{c}_1} + \frac{L_4}{\hat{c}_4 H_4} + 2\frac{\bar{f}_4}{\hat{c}_4}\right) \\ & + \ln\left(\frac{\hat{c}_4}{\hat{c}_1}\right). \end{aligned} \tag{31}$$

This equation can be written in a simpler and more intuitive manner

$$V = IR + V_0, \tag{32}$$

where R is the total resistance of the system and has been investigated in previous works [5,20] and the shifted potential [29,33] is

$$V_0 = \ln\left(\frac{\hat{c}_4}{\hat{c}_1}\right). \tag{33}$$

When this potential is applied, the inherent concentration gradients are countered leading to a new equilibrium state with $I = 0$. Equation (32) predicts that the current response about V_0 is antisymmetric, hence the I/V slope ratio between positive and negative current should be unity. As we will see in the results (Sec. III F) even at very small currents this ratio is not unity. This indicates that if one is interested in such a ratio, one should also account for the higher-order terms.

Rectification. It makes sense to define the rectification factor (*RF*) around the shifted electric potential

$$RF = \left|\frac{I_{V>V_0}}{I_{V<V_0}}\right|. \tag{34}$$

From this expression, it can be shown that current rectification does not only occur for the limiting currents but at all applied voltages. Rectification does not occur solely in an ideal permselective system but also in a nonideal permselective system. In the extreme case of vanishing permselectivity, we would still have a current-voltage response that was dependent only on the geometry and bulk concentrations, but there would be no rectification. In other words, the rectification occurs solely due to the symmetry-breaking property of ion permselectivity.

F. Results

We shall start investigating the behavior of asymmetric bulk concentrations. For the sake of simplicity we start by investigating the behavior of a simple 1D system with a symmetric geometry. In Fig. 2(a) we can see the effects of asymmetric bulk concentrations are manifested as shifts in the intersection of the $I-V$ curves and the $\hat{x}$ and $\hat{y}$ coordinates, change in the limiting current, and change in the slope (i.e., differential resistance). It can be observed that at high voltages, the current, calculated via numerical simulations, surpasses the limiting value. This stands in contrast to the above theoretical relations, which assume the LEN approximation and is due to the formation of the extended space-charge layer (SCL) [10,46] that is captured in the numerical simulations. While in the former case ε is identically zero, in the latter case it is small ($\varepsilon \ll 1$) but finite, thus, allowing for nonelectroneutrality to exist, capturing both the quasiequilibrium electric double layer (EDL) and the nonequilibrium SCL. As ε decreases so does the discrepancy [10,46]. In addition, ideal permselectivity is not *a priori* assumed by the numerical simulations. However, by taking $N \gg 1$ one can practically ensure that the coion concentration will be $O(N^{-1})$, which will also lead $j_- \simeq 0$. In Fig. 2(b) we demonstrate the behavior of the rectification factor. As we increased the asymmetry ratio in bulk concentrations we increased the range in which the rectification factor changes. Our theoretical predictions are confirmed by numerical simulations (details can be found in the Appendix).

In Fig. 3 we primarily investigate the case of symmetric bulk concentrations and microchamber geometries (the case of asymmetric microchamber geometries was covered in our previous work [5]) with an asymmetry in the permselective medium geometries. It can be seen that by increasing the ratio of the permselective medium heights (h_2/h_3), the rectification factor increases substantially. Our theoretical model thus qualitatively explains the previous experimental results of Yossifon *et al.* [43] where asymmetric nanochannel entrance geometries led to ionic current rectification due to concentration polarization. A quantitative comparison is not straightforward and necessitates accounting for additional effects existing in fabricated linear nanochannels, such as net electro-osmotic flow [47,48], surface conductance effects [11], and nonideal ion permselectivity [19,49] [$N \sim O(1)$], which are negligible in nanoporous membrane systems. We have also added a curve for the case of an asymmetric bulk concentrations and asymmetric permselective geometries (solid cyan line), which accounts for both kind of asymmetries and which is verified by simulations (red line with squares).

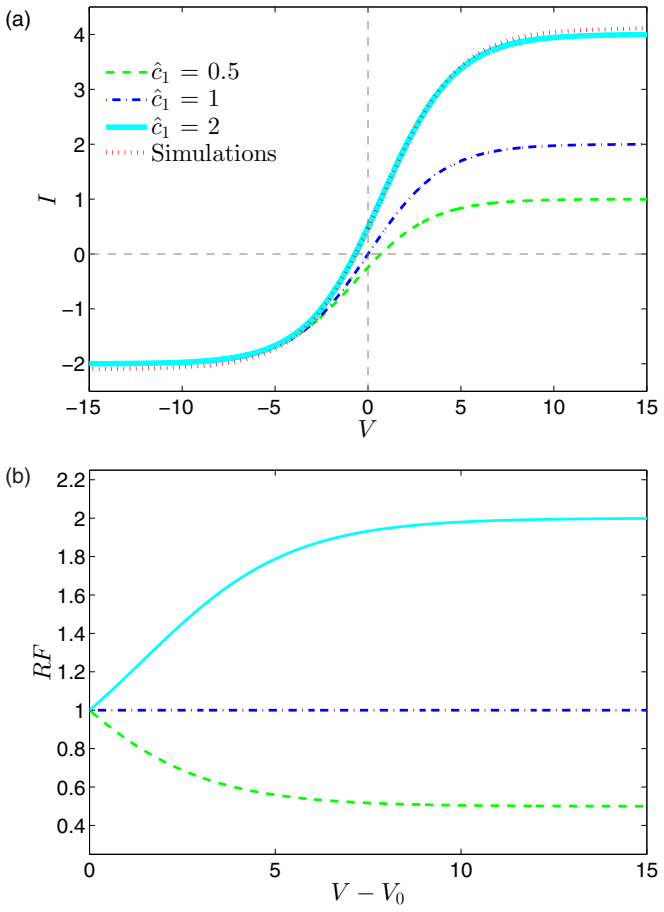

FIG. 2. (Color online) The (a) $I-V$ curves and (b) *RF* for a 1D system. All lengths scales are unity ($L_{1,4} = d_{2,3} = 1$) and $N_{2,3} = 10^2$. The bulk at $x = \Delta_4$ is kept constant $\hat{c}_4 = 1$, while the bulk concentration $\hat{c}_1$ is varied. The simulations were conducted for the following values: $L_{1,4} = d_{2,3} = 1$, $N_{2,3} = 10^2$, $\hat{c}_1 = 2$, $\hat{c}_4 = 1$, $\varepsilon = 10^{-4}$.

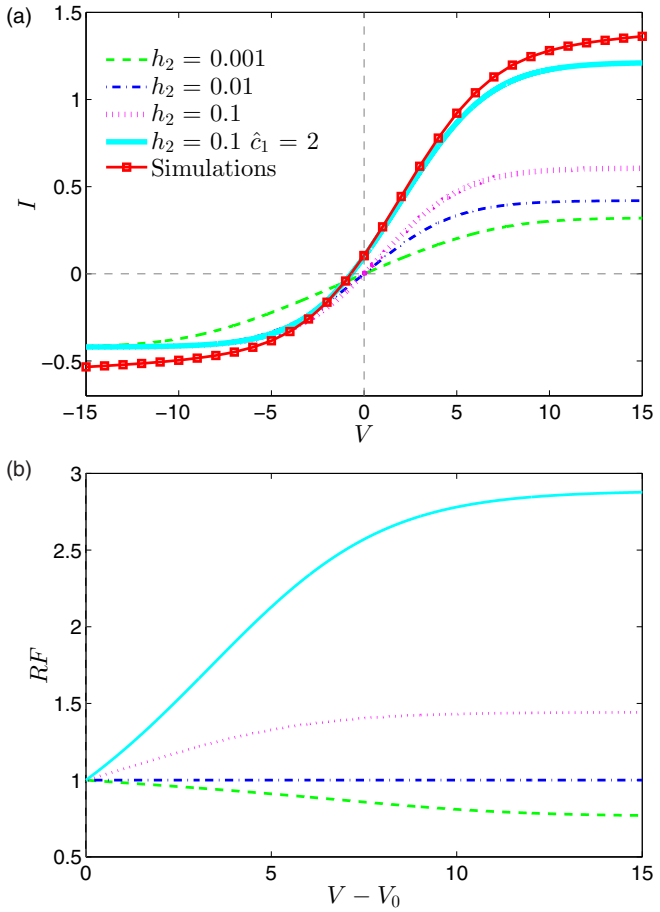

FIG. 3. (Color online) The (a) $I-V$ curves and (b) RF for a 2D system where the height h_2 was varied. All the length scales are unity ($L_{1,4} = d_{2,3} = 1$), while the remaining heights are $H_{1,4} = 0.4, h_3 = 10^{-2}$ and $N_{2,3} = 10^2$. The bulk at $x = \Delta_4$ is kept constant $\hat{c}_4 = 1$. The bulk concentration $\hat{c}_1 = 1$ unless otherwise specified. The simulations were conducted for the following values: $L_{1,4} = d_{2,3} = 1$, $H_{1,4} = 0.4$, $h_3 = 10^{-2}$, $N_{2,3} = 10^2$, $\hat{c}_4 = 1$, $\hat{c}_1 = 2$, $\varepsilon = 10^{-3}$. For the case of symmetric bulk concentrations $V_0 = 0$ while for the asymmetric case used here $V_0 = -\ln 2$.

IV. ASYMMETRIES IN THE ELECTRIC CHARGE OF THE PERMSELECTIVE REGIONS

Similar to the dialytic battery, a permselective-media-based bipolar diode, based on at least two permselective regions of opposite charges, is not only interesting from a physical point of view but also from an application point view. From as far back as the 1960s [50,51] bipolar membrane systems have been investigated. It was shown, qualitatively, that such systems display similar properties to P-N junction diodes encountered commonly in solid-state physics [52]. Perhaps the most interesting of these properties is the rectification capability exhibiting a preferred direction in the transport of current.

Sonin and Grossman [53] analyzed the complex system of four 1D permselective membranes adjacent to each other. Due to the complexity of such a system they made a number of oversimplifying assumptions, such as a linear concentration and electric potential profile within the permselective regions, which is not always as the case. Grossman [54] later followed up with a simpler two-layered model where he investigated the effects of water splitting on the $I-V$ response. While a detailed mathematical model was presented for four ionic species, due to its complexity, numerical analysis was eventually required. Since then, much work has been conducted on membrane systems [55,56] (see the recent review [57] and references therein). Unexpectedly, within the ever-growing field of nanofluidics, bipolar permselective nanochannels have also started to receive attention [41,58,59], however, little theoretical attention has been given to this subject. Additionally, the effects of two dimensions have not been investigated at all. However, a complete theoretical model of a bipolar diode consisting of a four-layered model (two microchambers and two permselective regions) has yet to be derived.

In this section we will discuss the case where N_2 and N_3 are not of the same sign and not necessarily of the same absolute value. We will systematically derive a $I-V$ relation as well as the 2D concentration and electric potential distributions under the assumption of local electroneutrality. Our $I-V$ relation will indeed predict the diodelike behavior.

In a four-layered system (Fig. 1) if we were to assume that each of the permselective regions were ideal, then we would reach the immediate and intuitive result that the cationic current through the anion region is zero, as well as the anionic current through the cation region is zero. Due to the requirement of current conservation this would lead to the trivial response that the overall current in the system is zero unless there is water splitting at the interface between the permselective mediums (which requires two additional species). This requires that we lift the beneficial constraint of ideality, which allowed us to derive a general solution without requiring any additional assumptions. As we shall shortly see, a different *ad hoc* assumption will be used to allow us to continue with an analytical derivation. The consequences of this assumption and its outcome will be discussed thoroughly.

A. Assumptions

Taking the sum and differences between Eqs. (1) and (2) gives two sets of equations

$$\nabla\cdot[\nabla(c_+ + c_-) + (c_+ - c_-)\nabla\phi] = -\nabla\cdot(\boldsymbol{j}_+ + \boldsymbol{j}_-) = -\nabla\cdot\boldsymbol{j} = 0, \tag{35}$$

$$\nabla\cdot[\nabla(c_+ - c_-) + (c_+ + c_-)\nabla\phi] = -\nabla\cdot(\boldsymbol{j}_+ - \boldsymbol{j}_-) = -\nabla\cdot\boldsymbol{i} = 0, \tag{36}$$

where $\boldsymbol{j}$ is the salt flux density (normalized by $\tilde{D}\tilde{c}_0/\tilde{L}$) and $\boldsymbol{i}$ the current flux density (normalized by $F\tilde{D}\tilde{c}_0/\tilde{L}$). Under the LEN approximation, $\rho_e = 0$, within the microchambers (regions 1 and 4) $c_+ = c_- = c$, hence

$$\nabla^2 c_k = -\tfrac{1}{2}\nabla\cdot\boldsymbol{j}_k = 0, \quad k = 1,4, \tag{37}$$

$$\nabla\cdot(c_k\nabla\phi_k) = -\tfrac{1}{2}\nabla\cdot\boldsymbol{i}_k = 0, \quad k = 1,4. \tag{38}$$

In permselective regions 2 and 3 we obtain similar equations, only now instead of requiring the assumption of LEN we require cross-sectional local electroneutrality

$$c_{+,l} - c_{-,l} = N_l, \quad l = 2,3, \tag{39}$$

and by defining $s_l = c_{+,l} + c_{-,l}$ ($l = 2,3$) one obtains

$$\nabla \cdot [\nabla s_l + N_l \nabla \phi_l] = -\nabla \cdot \boldsymbol{j}_l = 0, \tag{40}$$

$$\nabla \cdot [s_l \nabla \phi_l] = -\nabla \cdot \boldsymbol{i}_l = 0 \Rightarrow s_l \nabla \phi_l = -\boldsymbol{i}_l. \tag{41}$$

Let us analyze the vector components of $\boldsymbol{j}_l$ in Eq. (40). Due to the requirements that the walls are insulating $(\boldsymbol{j}_\pm \cdot \boldsymbol{y}) = 0$ means that $j_y = i_y = 0$ at the walls. A simplifying assumption would be that both the salt flux and current density are uniform within the permselective mediums. This reduces Eqs. (40) and (41) to be 1D (after dropping the x subscripts for the currents)

$$s_{lx} + N_l \phi_{lx} = -j_l, \tag{42}$$

$$s_l \phi_{lx} = -i_l. \tag{43}$$

In general one needs to find the $j-i$ relation for our four-layered problem. A similar problem was recently covered in the thorough work of abu-Rhal *et al.* [19], which investigated the effects of a single nonideal permselective region (three-layers system). It was shown there that one can find a nontrivial relation between $j-i$ that needs be to solved using Lambert functions and is evaluated numerically. In our case we can indeed derive a similar $j-i$ relation, however, we would then be unable to proceed with deriving a basic solution in term of closed functions. We have therefore chosen to make the following *ad hoc* assumption whose consequences will be discussed later on when they become more apparent

$$j_+ = -j_- \Rightarrow j = 0, \quad i = 2j_+. \tag{44}$$

The physical justification is based on the following heuristic argument. If we were to assume that the permselective regions are ideal, than as we have previously mentioned, the resultant current would be zero. By alleviating this requirement we are now allowing a small current to be created and transported through each of the regions. For reasons of symmetries, let us assume that this current is rather small and equal in magnitude. While this paper focuses on breaking numerous symmetries through the system including the sign of the surface charge, even by assuming a symmetry in the amplitude of the ionic current densities we shall soon witness that the system will behave in an inherently asymmetric manner.

B. Concentration solution

It is now quite easy to resolve the concentrations within the microchambers (region 1 and 4 [Eq. (37)]). The BCs given in Sec. III B remain the same with the sole difference that the BCs at the permselective interface changes [Eqs. (12) and (13) are now $c_{k,x}(x = \Delta_k, y) = 0, k = 1,3$]. Since $\boldsymbol{j} = \boldsymbol{0}$ from Eq. (37)

$$\nabla c_k = 0, \quad k = 1,4, \tag{45}$$

resulting in uniform concentrations within regions 1 and 4

$$c_1(x,y) = \hat{c}_1, \quad c_4(x,y) = \hat{c}_4. \tag{46}$$

Within the permselective regions 2 and 3 we solve the following equations

$$s_{lx} - N_l \frac{i_l}{s_l} = 0, \quad l = 2,3. \tag{47}$$

This Bernoulli-type differential equation has a solution

$$s_l(x) = \pm\sqrt{2 i_l N_l x + A_l}, \quad l = 2,3 \tag{48}$$

and since the concentration must be positive we take the positive branch, and A_l is an unknown constant to be found later. By using Eq. (39) we can rewrite this in term of the concentrations

$$c_{\pm,l}(x,y) = \frac{s_l \pm N_l}{2} = \frac{\sqrt{2 i_l N_l x + A_l} \pm N_l}{2}, \quad l = 2,3. \tag{49}$$

C. Electric potential solution

Substituting Eq. (48) into Eq. (43) yields

$$\phi_l = -\frac{\sqrt{2 i_l N_l x + A_l}}{N_l} + B_l, \quad l = 2,3. \tag{50}$$

We thus have four unknown constants of integration, which we would like to find $\{A_2, A_3, B_2, B_3\}$. To find these four unknowns requires continuity of the electrochemical potential [Eq. (15)] of both the anions and cations at the permselective mediums boundaries

$$\mu_{\pm,k}(x = \Delta_k, y = 0) = \mu_{\pm,k+1}(x = \Delta_k, y = 0), \quad k = 1,2,3. \tag{51}$$

Equation (51) constitutes six BCs while we have only four unknowns. Four of the equations will be solved for the unknowns while the fifth equation will give us the $I-V$ relation and the sixth relation will give us an additional constraint to our $j = 0$ assumption.

Prior to solving for the constants we provide the solution for the electric potential in regions 1 and 4. Now that the concentration distributions have been shown to be uniform, the governing equation [Eq. (38)] reduces to Laplace's equation

$$\nabla^2 \phi = 0. \tag{52}$$

The BCs for the electric potential still include a potential drop V over the entire system

$$\phi(x = 0, y) = V, \quad \phi(x = \Delta_4, y) = 0. \tag{53}$$

Requiring the electrical insulation at the microchamber walls and symmetry planes

$$\frac{\partial \phi}{\partial n} = 0. \tag{54}$$

This can be written explicitly as

$$\phi_y(x, H_k) = \phi_y(x, 0) = 0, \quad k = 1,4. \tag{55}$$

At the permselective surfaces located at $x = \Delta_1, \Delta_2, \Delta_3$ we continue with the simplifying assumption of uniform current density along the interface between the permselective medium

and the microchannels

$$\phi_x(x=\Delta_1,y)=\begin{cases}-I/(2h_2\hat{c}_1) & 0\leqslant y\leqslant h_2,\\ 0 & \text{otherwise},\end{cases}, \tag{56}$$

$$\phi_x(x=\Delta_3,y)=\begin{cases}-I/(2h_3\hat{c}_4) & 0\leqslant y\leqslant h_3,\\ 0 & \text{otherwise},\end{cases}, \tag{57}$$

$$@x=\Delta_2,\quad I=i_2h_2=i_3h_3. \tag{58}$$

Equation (58) represents the requirement that the total electric current is conserved at the interface $x=\Delta_2$ where a discontinuity exists in the geometries thus leading to different electric current densities i_2,i_3.

Since the governing equation and BCs for the electric potential in this part are identical to those for the concentration in the previous section (Sec. III), this suggests that the electric potential solutions have a similar form

$$\phi_1(x,y)=V-\frac{I}{2H_1\hat{c}_1}x-\frac{I}{\hat{c}_1h_2H_1}\sum_{n=1}^{\infty}\frac{\sin(\lambda_nh_2)}{\lambda_n^2\cosh(\lambda_nL_1)}\sinh(\lambda_nx)\cos(\lambda_ny), \tag{59}$$

$$\phi_4(x,y)=\frac{I}{2H_4\hat{c}_4}(\Delta_4-x)+\frac{I}{\hat{c}_4h_3H_4}\sum_{n=1}^{\infty}\frac{\sin(\kappa_nh_3)}{\kappa_n^2\cosh(\kappa_nL_4)}\sinh[\kappa_n(\Delta_4-x)]\cos(\kappa_ny). \tag{60}$$

Taking the sum of the anion and cation electrochemical potential [Eq. (15)] removes the dependency of the electric potential and one gets

$$(c_{+,k}c_{-,k})|_{x=\Delta_k}=(c_{+,k+1}c_{-,k+1})|_{x=\Delta_k},\quad k=1,2,3. \tag{61}$$

As it turns out this is optimal for the permselective concentrations due to their functional form [Eq. (49)]. At $x=\Delta_1,\Delta_3$ this gives

$$A_2=4\hat{c}_1^2+{N_2}^2-2\frac{I}{h_2}N_2L_1, \tag{62}$$

$$A_3=4\hat{c}_4^2+{N_3}^2-2\frac{I}{h_3}N_3\Delta_3. \tag{63}$$

The condition at $x=\Delta_2$ gives the following condition that needs to be met

$$4\hat{c}_1^2+2I\frac{N_2d_2}{h_2}=4\hat{c}_4^2-2I\frac{N_3d_3}{h_3}. \tag{64}$$

Such a constraint, which has a dependence on the current, can only be met if the bulk concentrations are symmetric to negate the current dependency. Hence, another disadvantage to assume that $j=0$ is that we cannot solve for the most general problem, which also includes asymmetries in the bulk concentrations, but we now have a very simple constraint for the bulk concentrations, geometries, and counterion concentrations

$$\hat{c}_1=\hat{c}_4=1 \tag{65}$$

$$\frac{|N_2|d_2}{h_2}=\frac{|N_3|d_3}{h_3}. \tag{66}$$

By solving for the $j\neq 0$ case and finding the $j-i$ relation, the asymmetric bulk concentrations can also be accounted for but this shall be left for future work. We shall now find our two additional constants and $I-V$ relation by using either the positive or negative electrochemical potential at $x=\Delta_1,\Delta_2,\Delta_3$. We use the positive electrochemical potential. The BCs at $x=\Delta_1,\Delta_3$ yield [including substitution of Eqs. (62) and (63)]

$$B_2=V-I\left(\frac{L_1}{2H_1}+\bar{f}_1\right)+\frac{\bar{Q}_2}{N_2}-\ln\left[\frac{\bar{Q}_2+N_2}{2}\right], \tag{67}$$

$$B_3=I\left(\frac{L_4}{2H_4}+\bar{f}_4\right)+\frac{\bar{Q}_3}{N_3}-\ln\left[\frac{\bar{Q}_3+N_3}{2}\right] \tag{68}$$

with

$$\bar{Q}_l=\sqrt{4+{N_l}^2}. \tag{69}$$

Finally we use the BC at $x=\Delta_2$ and derive the $I-V$ relation

$$V=I\left(\frac{L_1}{2H_1}+\bar{f}_1+\frac{L_4}{2H_4}+\bar{f}_4\right)+\left(\frac{\bar{Q}_3}{N_3}-\frac{S_{-,3}}{N_3}-\frac{\bar{Q}_2}{N_2}+\frac{S_{+,2}}{N_2}\right)+\ln\left[\left(\frac{S_{-,3}+N_3}{\bar{Q}_3+N_3}\right)\left(\frac{\bar{Q}_2+N_2}{S_{+,2}+N_2}\right)\right], \tag{70}$$

with

$$S_{\pm,l}=\sqrt{4+{N_l}^2\pm2\frac{I}{h_l}N_ld_l}. \tag{71}$$

The $I-V$ relation given by Eq. (70) is comprised of three different terms. The first term accounts for the microchambers' Ohmic resistors, which also account for field focusing into the permselective interfaces. The second term describes the potential drop over the permselective regions. The third term describes the Donnan potential jumps at all three interfaces.

D. Bipolar behavior

While Eq. (70) has a complicated form, there remains a lot of interesting physics that appear hidden but are in fact quite apparent. To show this we shall start off by analyzing the 1D case ($H_{1,4}=h_{2,3}$, $I/h\to i$) with an additional simplifying assumption of equal length scales ($L_{1,4}=d_{2,3}=L$). Under the constraint of Eq. (66) we have that $N_2=-N_3=N$. For this case we see that $\bar{Q}_2=\bar{Q}_3$ and $S_{+2}=S_{-3}$. Also we shall assume $N\gg 1$ or that counterion charge is large relative to other properties, which will be defined as needed. Thus Eq. (70) reduces to

$$V=iL+\frac{2}{N}(S_{+,2}-\bar{Q}_2)+\ln\left[\left(\frac{S_{+,2}-N}{\bar{Q}_2-N}\right)\left(\frac{\bar{Q}_2+N}{S_{+,2}+N}\right)\right]. \tag{72}$$

The second term can be written in the following manner

$$\begin{aligned} S_{+,2} - \bar{Q}_2 &= \bar{Q}_2\left(\frac{S_{+,2}}{\bar{Q}_2} - 1\right) \\ &= \bar{Q}_2\left(\sqrt{\frac{4+N^2+2iNL}{4+N^2}} - 1\right) \\ &\overset{N\gg 1}{\approx} N\left(\sqrt{1+\frac{2iL}{N}} - 1\right) \overset{|i|\ll N/L}{\approx} iL. \end{aligned} \quad (73)$$

Prior to the simplification $|i| \ll N/L$, we see that this expression is not symmetric with i as there are no limits on positive values but there is a limit on the negative value, $i > -N/2L$. Under the simplification $|i| \ll N/L$, we see that the second term, associated with the permselective medium, behaves as an Ohmic resistor with a resistance that is $O(1/N)$ smaller than that of the microchamber resistance.

It is the third term that is the most interesting. Inserting the $S_{+,2}$ and $\bar{Q}_2$ functions and looking at the case of $N \gg 1$ and $|i|NL \ll 1$ one can look at an expansion of the

$$\ln\left[\left(\frac{S_{+2}-N}{\bar{Q}_2-N}\right)\left(\frac{\bar{Q}_2+N}{S_{+,2}+N}\right)\right] \approx \ln\left[1+\frac{iNL}{2}\right]. \quad (74)$$

Such a resistor is clearly asymmetric with the current and will result in rectification. Once more, there is no upper bound on the positive currents while the negative current has a limiting value of $i_{\rm lim} = -2/NL$ due to the constraint $(S_{+2} - N) > 0$. This constraint is more restrictive than the previous constraint $(i > -N/2L)$. In two dimensions $(h_{2,3} = h,\ N_2 = -N_3 = N)$, the former constraint translates into $I_{\rm lim} = -2h/NL$. The asymmetric and diodelike behavior of the current is due to the system layout. When the voltage is applied in the direction that coincides with the inherent electric field of positive N to negative N then the current is enhanced. The reason that there is no limiting current in this forward bias is because we have forgone the assumption of ideal permselectivity. When the voltage is applied in the opposite direction, reverse bias, then the applied electric field is operating against the inherent electric field. This leads to a reduction in the resultant current.

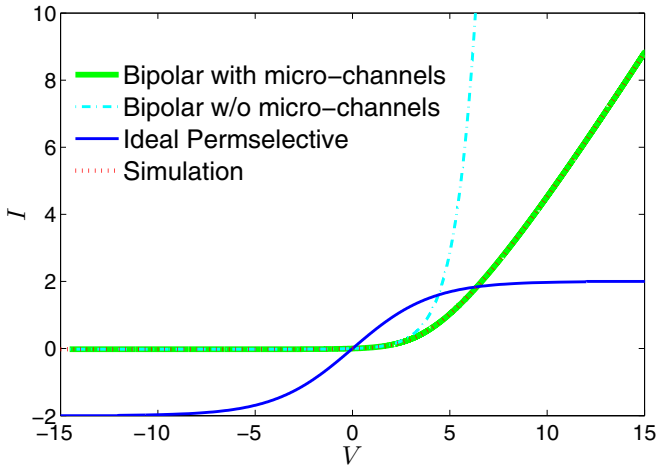

FIG. 4. (Color online) The $I-V$ curves for a 1D system. All lengths scales are unity $(L_{1,4} = d_{2,3} = 1)$ and $N_2 = -N_3 = 10^2$. For the sake of comparison we have added the positive branch of the $I-V$ for an ideal permselective system with $N_{2,3} = 10^2$. The simulations were conducted for the following values: $L_{1,4} = d_{2,3}$=1, $N_2 = -N_3 = 10^2$, $\hat{c}_4 = 1$, $\hat{c}_1 = 1$, $\varepsilon = 10^{-4}$.

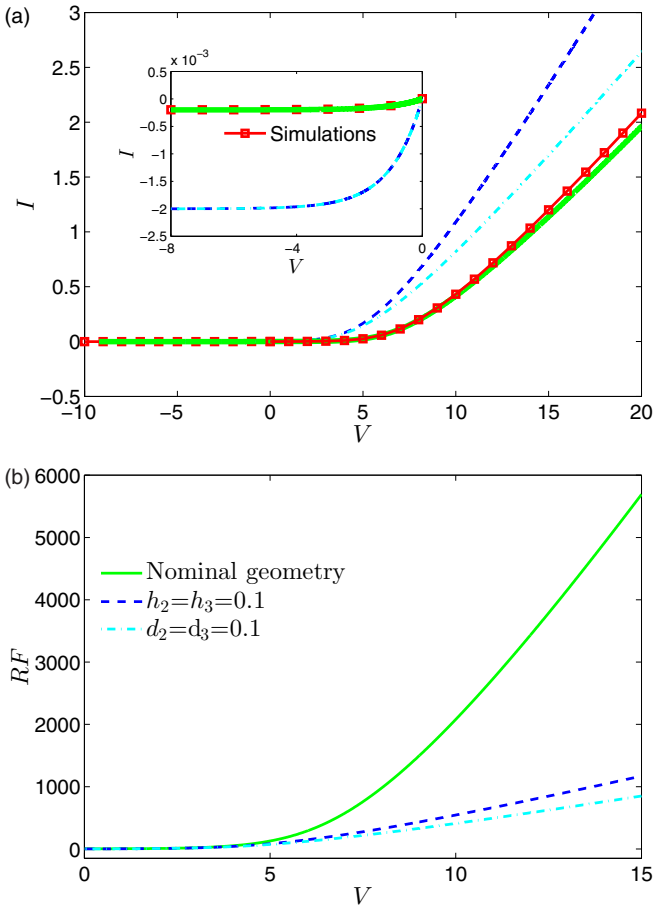

FIG. 5. (Color online) The (a) $I-V$ curves and (b) RF for a 2D system where the geometry is varied. The nominal geometry is such that the length of each region is unity $(L_{1,4} = d_{2,3} = 1)$ and the heights are $H_{1,4} = 0.4$, $h_{2,3} = 10^{-2}$. For all curves a value of $N_2 = -N_3 = 10^2$ was used. The simulations (red squares) were conducted for the following values: $L_{1,4} = d_{2,3} = 1$, $H_{1,4} = 0.4$, $h_{2,3} = 10^{-2}$, $N_2 = -N_3 = 10^2$, $\hat{c}_{1,4} = 1$, $\varepsilon = 10^{-3}$.

E. Analysis and key results

In Fig. 4 we plot the $I-V$ for a 1D system where all the length scales are unity. Theoretical predictions are verified by simulations. For the sake of comparison we have added two curves: (i) the response of a system without the microchambers and (ii) the response of an ideal permselective systems whose geometry is identical and $N_2 = N_3$. It is observed that the microchamber reduces the overall current, in a non-negligible manner, due to an increase the overall resistance. Hence, one should not unequivocally neglect the effects of the microchambers. Additionally, we see that the nonideal forward bias (i.e., $V > 0$) does not have a limiting current as the ideal case does. In contrast, the nonideal reverse biased (i.e., $V < 0$) current's absolute value is substantially lower than the ideal case (whose limiting value is 2).

In Fig. 5 we investigate the 2D behavior of the system by changing a number of geometric properties. First and foremost, it is visible that the response changes substantially with the geometry. By increasing the height or decreasing length of the system, we are decreasing the overall resistance. Moreover, we see that the rectification factor can now be on the order of magnitude of $O(10^2$–$10^3)$ whereas in the 1D case (which is not plotted) one gets a RF value of $O(10^2)@10V$. Indeed as the geometry changed, so did the limiting current $I = -2h/Nd$, which also resulted in the change of the RF (see inset). Also by observing the change in the slope of the RF one gets a good qualitative understanding when the diode behavior comes into play (this becomes more visible in a semilog plot, which is not shown here).

V. CONCLUSIONS

This work focuses on additional asymmetries (bulk concentrations, geometric, and surface charge properties) in permselective systems that possess an inherently symmetry-breaking property. These asymmetries eventually lead to the electrical current rectification.

In Sec. III we derived a general solution for a dialytic battery where both permselective regions were of the same charge. We showed that any bulk concentration asymmetry allows for the harvesting of electrical energy. In addition we showed that based on this asymmetry and geometric asymmetries, the current has a preferred direction for transport resulting in current rectification.

In Sec. IV we investigated the bipolar behavior of systems whose permselective regions have an opposite charge. We are able to derive an $I-V$ response under an additional *ad hoc* assumption. Due to the surface charge asymmetry one can design a simple nanofluidic-based diode whose rectification (depends on the geometry) can be as large as 10^2-10^3.

ACKNOWLEDGMENTS

This work was supported by ISF Grant No. 1078/10. We thank the Technion RBNI (Russell Berrie Nanotechnology Institute) and the Technion GWRI (Grand Water Research Institute) for their financial support.

APPENDIX: NUMERICAL SIMULATIONS

To verify our results we solved the fully coupled PNP equations given by Eqs. (1)–(3) using the finite elements program COMSOL™ for the two-dimensional geometry described in Fig. 1. The PNP equations were solved using the Transport of Diluted Species and Electrostatic modules in COMSOL.

The 1D and 2D scenarios were solved separately. The reason is as follows. For a truly 1D system (i.e., solving the problem on a 1D straight line) the numerics are very simple. All that is required is to resolve the Debye length whose structure is 1D and behavior is rather simple [10,46]. Usually 10^3 elements within this small region of order 10ε is all that is required. Outside of the Debye length, the resolution of the mesh can be rather coarse. Most computers nowadays can easily handle several thousand elements (and degrees of freedom) and provide almost instantaneous answers. Thus we used a very small value of $\varepsilon = 10^{-4}$ for 1D simulations.

In contrast, in 2D simulations, to resolve the 2D structure of the Debye length the mesh needs to resolve a region whose height is approximately h. Thus the number of elements (and degrees of freedom) needs to be multiplied by a factor of h/ε making numerical simulations very expensive. Due to the fact this problem is singular with ε and 2D realistically being quite expensive to solve numerically, the advantage of solving the problem using our theoretical approach, which is equivalent to taking $\varepsilon \to 0$, becomes even more apparent. In our 2D simulations we used $\varepsilon = 10^{-3}$. While we find COMSOL a convenient program to solve the PNP equations to get an answer very quickly, it has been recently shown that customized codes can be more efficient for the study of PNP in conjunction with hydrodynamic effects [60].

[1] V. G. Levich, *Physicochemical Hydrodynamics* (Prentice-Hall, New York, 1962).
[2] I. Rubinstein, *Electro-Diffusion of Ions* (SIAM, Philadelphia, 1990).
[3] D. Stein, M. Kruithof, and C. Dekker, Surface-Charge-Governed ion Transport in Nanofluidic Channels, Phys. Rev. Lett. **93**, 035901 (2004).
[4] R. B. Schoch, H. van Lintel, and P. Renaud, Effect of the surface charge on ion transport through nanoslits, Phys. Fluids **17**, 100604 (2005).
[5] Y. Green, S. Shloush, and G. Yossifon, Effect of geometry on concentration polarization in realistic heterogeneous permselective systems, Phys. Rev. E **89**, 043015 (2014).
[6] I. Rubinstein, Electroconvection at an electrically inhomogeneous permselective interface, Phys. Fluids A **3**, 2301 (1991).
[7] Y. Green, and G. Yossifon, Effects of three-dimensional geometric field focusing on concentration polarization in a heterogeneous permselective system, Phys. Rev. E **89**, 013024 (2014).
[8] V. V. Nikonenko, A. V. Kovalenko, M. K. Urtenov, N. D. Pismenskaya, J. Han, P. Sistat, and G. Pourcelly, Desalination at overlimiting currents: State-of-the-art and perspectives, Desalination **342**, 85 (2014).
[9] N. A. Mishchuk, Concentration polarization of interface and non-linear electrokinetic phenomena, Adv. Colloid Interface Sci. **160**, 16 (2010).
[10] I. Rubinstein and L. Shtilman, Voltage against current curves of cation exchange membranes, J. Chem. Soc., Faraday Trans. 2 **75**, 231 (1979).
[11] E. V. Dydek, B. Zaltzman, I. Rubinstein, D. S. Deng, A. Mani, and M. Z. Bazant, Overlimiting Current in a Microchannel, Phys. Rev. Lett. **107**, 118301 (2011).
[12] A. Mani and M. Z. Bazant, Deionization shocks in microstructures, Phys. Rev. E **84**, 061504 (2011).

[13] I. Rubinstein and B. Zaltzman, Electro-osmotically induced convection at a permselective membrane, Phys. Rev. E **62**, 2238 (2000).
[14] B. Zaltzman and I. Rubinstein, Electro-osmotic slip and electroconvective instability, J. Fluid Mech. **579**, 173 (2007).
[15] S. S. Dukhin, Electrokinetic phenomena of the second kind and their applications, Adv. Colloid Interface Sci. **35**, 173 (1991).
[16] H.-C. Chang, E. A. Demekhin, and V. S. Shelistov, Competition between Dukhin's and Rubinstein's electrokinetic modes, Phys. Rev. E **86**, 046319 (2012).
[17] Y. Green and G. Yossifon, Dynamical trapping of colloids at the stagnation points of electro-osmotic vortices of the second kind, Phys. Rev. E **87**, 033005 (2013).
[18] A. Yaroshchuk, E. Zholkovskiy, S. Pogodin, and V. Baulin, Coupled Concentration Polarization and Electroosmotic Circulation near Micro/Nanointerfaces: Taylor-Aris Model of Hydrodynamic Dispersion and Limits of Its Applicability, Langmuir **27**, 11710 (2011).
[19] R. abu-Rjal, V. Chinaryan, M. Z. Bazant, I. Rubinstein, and B. Zaltzman, Effect of concentration polarization on permselectivity, Phys. Rev. E **89**, 012302 (2014).
[20] Y. Green and G. Yossifon, Time-dependent ion transport in heterogeneous permselective systems, Phys. Rev. E **91**, 063001 (2015).
[21] I. Rubinstein and B. Zaltzman, Equilibrium Electroconvective Instability, Phys. Rev. Lett. **114**, 114502 (2015).
[22] R. B. Schoch and P. Renaud, Ion transport through nanoslits dominated by the effective surface charge, Appl. Phys. Lett. **86**, 253111 (2005).
[23] Y. Green, S. Park, and G. Yossifon, Bridging the gap between an isolated nanochannel and a communicating multipore heterogeneous membrane, Phys. Rev. E **91**, 011002(R) (2015).
[24] S. J. Kim, Y.-C. Wang, J. H. Lee, H. Jang, and J. Han, Concentration Polarization and Nonlinear Electrokinetic Flow near a Nanofluidic Channel, Phys. Rev. Lett. **99**, 044501 (2007).
[25] G. Yossifon, P. Mushenheim, Y.-C. Chang, and H.-C. Chang, Eliminating the limiting-current phenomenon by geometric field focusing into nanopores and nanoslots, Phys. Rev. E **81**, 046301 (2010).
[26] R. Chein and B. Chung, Numerical study of ionic current rectification through non-uniformly charged micro/nanochannel systems, J. Appl. Electrochem. **43**, 1197 (2013).
[27] J. D. Sherwood, M. Mao, and S. Ghosal, Electroosmosis in a Finite Cylindrical Pore: Simple Models of End Effects, Langmuir **30**, 9261 (2014).
[28] R. E. Pattle, Production of Electric Power by mixing Fresh and Salt Water in the Hydroelectric Pile, Nature (London) **174**, 660 (1954).
[29] J. N. Weinstein and F. B. Leitz, Electric Power from Differences in Salinity: The Dialytic Battery, Science **191**, 557 (1976).
[30] R. S. Norman, Water Salination: A Source of Energy, Science **186**, 350 (1974).
[31] D. Brogioli, Extracting Renewable Energy from a Salinity Difference Using a Capacitor, Phys. Rev. Lett. **103**, 058501 (2009).
[32] F. La Mantia, M. Pasta, H. D. Deshazer, B. E. Logan, and Y. Cui, Batteries for Efficient Energy Extraction from a Water Salinity Difference, Nano Lett. **11**, 1810 (2011).
[33] B. B. Sales, M. Saakes, J. W. Post, C. J. N. Buisman, P. M. Biesheuvel, and H. V. M. Hamelers, Direct Power Production from a Water Salinity Difference in a Membrane-Modified Supercapacitor Flow Cell, Environ. Sci. Technol. **44**, 5661 (2010).
[34] P. Długołęcki, A. Gambier, K. Nijmeijer, and M. Wessling, Practical Potential of Reverse Electrodialysis As Process for Sustainable Energy Generation, Environ. Sci. Technol. **43**, 6888 (2009).
[35] F. Suda, T. Matsuo, and D. Ushioda, Transient changes in the power output from the concentration difference cell (dialytic battery) between seawater and river water, Energy **32**, 165 (2007).
[36] E. Brauns, Salinity gradient power by reverse electrodialysis: effect of model parameters on electrical power output, Desalination **237**, 378 (2009).
[37] E. Brauns, Towards a worldwide sustainable and simultaneous large-scale production of renewable energy and potable water through salinity gradient power by combining reversed electrodialysis and solar power?, Desalination **219**, 312 (2008).
[38] S. Pacala and R. Socolow, Stabilization Wedges: Solving the Climate Problem for the Next 50 Years with Current Technologies, Science **305**, 968 (2004).
[39] P. Moriarty and D. Honnery, Hydrogen's role in an uncertain energy future, Int. J. Hydrogen Energy **34**, 31 (2009).
[40] L.-J. Cheng and L. J. Guo, Rectified Ion Transport through Concentration Gradient in Homogeneous Silica Nanochannels, Nano Lett. **7**, 3165 (2007).
[41] L.-J. Cheng and L. J. Guo, Ionic Current Rectification, Breakdown, and Switching in Heterogeneous Oxide Nanofluidic Devices, ACS Nano **3**, 575 (2009).
[42] W. Guo, L. Cao, J. Xia, F.-Q. Nie, W. Ma, J. Xue, Y. Song, D. Zhu, Y. Wang, and L. Jiang, Energy Harvesting with Single-Ion-Selective Nanopores: A Concentration-Gradient-Driven Nanofluidic Power Source, Adv. Funct. Mater. **20**, 1339 (2010).
[43] G. Yossifon, Y.-C. Chang, and H.-C. Chang, Rectification, Gating Voltage, and Interchannel Communication of Nanoslot Arrays due to Asymmetric Entrance Space Charge Polarization, Phys. Rev. Lett. **103**, 154502 (2009).
[44] J.-Y. Jung, P. Joshi, L. Petrossian, T. J. Thornton, and J. D. Posner, Electromigration Current Rectification in a Cylindrical Nanopore Due to Asymmetric Concentration Polarization, Anal. Chem. **81**, 3128 (2009).
[45] I. Rubinstein, B. Zaltzman, and T. Pundik, Ion-exchange funneling in thin-film coating modification of heterogeneous electrodialysis membranes, Phys. Rev. E **65**, 041507 (2002).
[46] E. Yariv, Asymptotic current-voltage relations for currents exceeding the diffusion limit, Phys. Rev. E **80**, 051201 (2009).
[47] J. Schiffbauer, and G. Yossifon, Role of electro-osmosis in the impedance response of microchannel-nanochannel interfaces, Phys. Rev. E **86**, 056309 (2012).
[48] J. Schiffbauer, S. Park, and G. Yossifon, Electrical Impedance Spectroscopy of Microchannel-Nanochannel Interface Devices, Phys. Rev. Lett. **110**, 204504 (2013).
[49] J. Schiffbauer, N. Leibowitz, and G. Yossifon, Extended space charge near nonideally selective membranes and nanochannels, Phys. Rev. E **92**, 013002 (2015).
[50] A. Mauro, Space Charge Regions in Fixed Charge Membranes and the Associated Property of Capacitance, Biophys J. **2**, 179 (1962).

[51] H. G. L. Coster, A Quantitative Analysis of the Voltage-Current Relationships of Fixed Charge Membranes and the Associated Property of 'Punch-Through', Biophys. J. **5**, 669 (1965).
[52] C. Kittel, *Introduction to Solid State Physics* (Wiley, New York, 1986).
[53] A. A. Sonin and G. Grossman, Ion transport through layered ion exchange membranes, J. Phys. Chem. **76**, 3996 (1972).
[54] G. Grossman, Water dissociation effects in ion transport through composite membrane, J. Phys. Chem. **80**, 1616 (1976).
[55] R. Simons and G. Khanarian, Water dissociation in bipolar membranes: Experiments and theory, J. Membrain Biol. **38**, 11 (1978).
[56] S. Mafé, J. A. Manzanares, and P. Ramirez, Model for ion transport in bipolar membranes, Phys. Rev. A **42**, 6245 (1990).
[57] Z. Slouka, S. Senapati, and H.-C. Chang, Microfluidic Systems with Ion-Selective Membranes, Ann. Rev. Anal. Chem. **7**, 317 (2014).
[58] H. Daiguji, Y. Oka, and K. Shirono, Nanofluidic Diode and Bipolar Transistor, Nano Lett. **5**, 2274 (2005).
[59] I. Vlassiouk and Z. S. Siwy, Nanofluidic Diode, Nano Lett. **7**, 552 (2007).
[60] E. Karatay, C. L. Druzgalski, and A. Mani, Simulation of chaotic electrokinetic transport: Performance of commercial software versus custom-built direct numerical simulation codes, J. Colloid Interface Sci. **446**, 67 (2015).